as far as connective tissue leucine aminopeptidase is concerned. Heat, organic solvents, and proteolytic enzymes readily deactivate the enzyme. The tightness of native protein molecules accounts largely for its resistance toward proteolytic enzymes. Comparing the adsorbed enzyme with the controls it appears that in the process of adsorption parts of the protein become sufficiently distorted to expose areas susceptible to proteolytic attack by trypsin and α-chymotrypsin. The distortions, however, do not include the active site since the activity is not impaired.

In contrast to the instability at higher temperatures the calcium phosphate gel–leucine aminopeptidase complex is very stable at 4° and in the presence of substrate at 40°. A single 0.5-mm thick calcium phosphate–leucine aminopeptidase membrane was used for many experiments over a 1-year period without a detectable loss of activity.

The potential usefulness of adsorbed leucine aminopeptidase for sequence analysis has been demonstrated. Using thicker layers of the enzyme the reaction speed can be adjusted to obtain sequences of small peptides in a time span dependent only upon the detection method used (1 hr for thin-layer chromatography). The filtrate can be analyzed by any method without pretreatment (deproteinization) at any enzyme/substrate ratio. The solid "leucine aminopeptidase reactor" is potentially useful in peptide analysis systems where continuous hydrolysis of part of the eluate is desired.

One aspect of biological interest is the great affinity of the connective tissue leucine aminopeptidase for calcium phosphate. Since the enzyme is extracted from a calcifying tissue the question arises whether the bound leucine aminopeptidase is the physiologic form rather than the soluble enzyme. The very high affinity for calcium phosphate appears to be unique for the connective tissue enzyme according to preliminary experiments.

References

Hornby, W. E., Lilly, M. D., and Crook, E. M. (1966), *Biochem. J. 98*, 420.

Jenkins, W. T. (1962), *Biochem. Prepn. 9*, 84.

Levin, Y., Pecht, M., Goldstein, L., and Katchalski, E. (1964), *Biochemistry*, *3*, 1905.

Matheson, A. T., and Tattri, B. L. (1964), *Can. J. Biochem. 42*, 95.

Schwabe, C. (1969), *Biochemistry 8*, 783 (this issue, preceding paper).

Weetall, H., and Weliky, N. (1969), Jet Propulsion Laboratory Space Programs Summary No. 37–26, Vol. IV, p 160.

Hydrolysis of Nucleoside Triphosphates by Myosin during the Transient State*

Birdwell Finlayson† and Edwin W. Taylor‡

ABSTRACT: The production of hydrogen ions during the hydrolysis of nucleotide triphosphates by myosin was determined in a stopped-flow spectrophotometer by measuring the optical density change of an indicator dye. At pH 8, in 0.5 M KCl with MgATP, MgITP, or CaATP as substrates, hydrogen ions were liberated during the transient phase at rates which greatly exceeded the steady-state rates of hydrolysis. The time course for MgATP at 0° or MgITP at 20° could be fitted by a single rate constant, while two rate constants were required for MgATP at 20° and CaATP at 0°.

In the case of MgATP at 20°, both rate constants were proportional to substrate concentration over a range of low substrate concentrations. As substrate concentration was increased above 10^{-4} M the rates approached limiting values corresponding to rate constants of approximately 130 and 20 sec^{-1}.

Numerous studies have been made of the enzymatic properties of myosin but with few exceptions (Nanninga and Mommaerts, 1960; Kanazawa and Tonomura, 1965; Tokiwa and Tonomura, 1965; Imamura *et al.*, 1965) analyses of the kinetics have been restricted to the steady-state behavior.

The production of hydrogen ions during hydrolysis of nucleotide triphosphates at pH 8 was determined by measuring the change in optical density of an indicator dye in a stopped-flow spectrophotometer.

---

* From the Department of Biophysics, University of Chicago, Chicago, Illinois. *Received June 11, 1968.*

† Present address: Department of Urology, University of Florida, Gainesville, Fla. The recipient of a Special Fellowship from the U. S. Public Health Service.

‡ This study was supported by a U. S. Public Health Service Research Grant, GM 10992. The recipient of a Research Career Development award from the U. S. Public Health Service.

An initial proton liberation which greatly exceeded the steady-state rate, was found for MgATP, MgITP, and CaATP. Examination of the kinetics as a function of substrate concentration indicated the presence of one or two proton-liberating steps, depending upon substrate and temperature. It was not possible to distinguish between a configuration charge or bond hydrolysis as the origin of the protons.

Materials and Methods

Preparation of Myosin. Male rabbits were sedated with barbiturate, paralyzed with intravenous administration of $MgCl_2$, and exsanguinated. The hind leg and paravertebral muscles below the thorax were used as starting material. Myosin was prepared by the method of Holtzer and Lowey (1959) except that precipitation was accomplished by dialysis against ten volumes of distilled water rather than dilution, in order to increase the yield. Preparations were occasionally examined by ultracentrifugation in the Spinco Model E centrifuge. Fresh preparations showed a single hypersharp peak. Prior to use, solutions were clarified by sedimentation at 66,000*g* for 45 min.

Protein concentration was determined from the difference in optical density at 291 and 350 mμ in 0.5 M NaOH (1 mg/ml = 0.735 optical density unit). The method was calibrated gravimetrically by dialyzing myosin solutions against deionized water followed by lyophilization and heating of the residue for 12 hr at 85°. Optical densities were determined in a Cary 14 spectrophotometer, employing a thermoregulated cell holder.

Glassware was extensively rinsed with deionized water and centrifugations were carried out in polycarbonate tubes to avoid contact with metals during preparation procedures.

Preparation of Reagents and Chemical Determinations. o-Creosol sulfonephthalein (Eastman Organic Chemicals) was dissolved in 0.5 M KCl and the pH adjusted with KOH. ATP (Pabst Brewing Co.) was used without purification. Solutions were made just prior to the experiments or were stored at −20°.

$CaCl_2$ solutions were made by dissolving $CaCO_3$ in an equivalent concentration of HCl in 0.5 M KCl followed by stirring for 12 hr under CO_2-free N_2. Solutions were subsequently adjusted to pH 6 with KOH.

All reagent solutions were degassed for at least 2 hr under reduced pressure using a water aspirator pump. Dye solutions were maintained at reduced pressure for 18 hr at pH 6.5, to remove dissolved CO_2. All subsequent manipulations of the reagents were made in a chamber flushed with CO_2-free N_2 and solutions were finally transferred to B-D Plastipak syringes. The loading port of the stopped-flow apparatus was designed to take these syringes so that solutions could be introduced into the apparatus without exposure to air.

Phosphate was determined by the Tausky and Shorr (1953) method. pH was measured in a thermoregulated cell and flushed with CO_2-free N_2 when necessary, employing a Sargent LS pH meter or Radiometer M-4 pH meter.

Stopped-Flow Spectrophotometer. The apparatus is based on design principles discussed by various authors (Gibson and Milnes, 1964; Sturtevant, 1963) and will not be described in great detail.

The basic features are illustrated schematically in Figures 1 and 2. Reactants from the two 1-ml tuberculine syringes are driven through a Gibson four-hole mixer (Gibson and Milnes, 1964) and a quartz observation tube, 2-mm internal diameter, and passed *via* a 14-gauge B-D stainless steel needle to a 5-ml Luer-lock syringe.

A Lucite block thermostated by circulating water holds the drive syringes, two 25-ml reservoir syringes, and a delrin valve system which permits reloading of the drive syringes. The reservoir syringes are loaded by attachment to the value system of 25-ml plastic syringes containing CO_2-free reagents.

The observation tube is contained in a copper block, in which four viewing slits are cut at right angles. Each quadrant is perforated with three holes for circulating fluid from a temperature bath. The drive syringes are powered by a rack and pinion coupled by an electromagnetic clutch to a one-fourth horsepower motor. At its highest position the drive plate is cocked by the lever of a microswitch which activates the electromagnetic clutch. A second microswitch is activated by the plunger of the stop syringe. A spring on the drive plate makes contact with a wire-wound resistor which functions as a voltage divider. The position and velocity of the drive plate is determined by displaying the output of the voltage divider on one channel of the oscilloscope.

Light from a tungsten or deuterium lamp of a Beckman DU monochromator is focused on the observation tube by a quartz lens. The transmitted beam passes through a collimating tube to a photomultiplier. The signal is fed through an emitter follower circuit to a Tektronix 3A3 differential amplifier and displayed on a Tektronic 564 storage screen oscilloscope using a 2B67 time base. The oscilloscope sweep can be triggered by either the start or stop microswitch. The emitter follower and oscilloscope trigger circuits were designed by Mr. R. Dykstra, Department of Chemistry, University of Chicago.

A more complete description of the apparatus can be obtained on request.

The flow velocity can be varied from 0 to 33 m sec^{-1} for solutions of viscosity 1 cP. Velocities are calculated from the slope of the trace recording the velocity of the drive plate and the ratio of cross-sectional areas of drive syringes and observation tube. The minimum delivery time from the mixer to the observation tube is 1 msec. Figure 3 shows optical density changes in the dehydration of carbonic acid by HCl using bromophenol blue as pH indicator. The oscilloscope has been triggered on start to illustrate events during the drive stroke. The initial drop in voltage represents the washing out of solution in the observation tube, plus any mixing lag during acceleration of the drive block. The constant optical density during much of the drive stroke indicates that mixing is complete long before flow stops.

The behavior of the instrument as a spectrophotometer was tested and Beer's law was obeyed at 590 mμ (bromophenol blue) and 350 mμ (colchicine) for concentrations in the range from 0 to 10^{-4} M. The equivalent absorption path length is 0.185 cm.

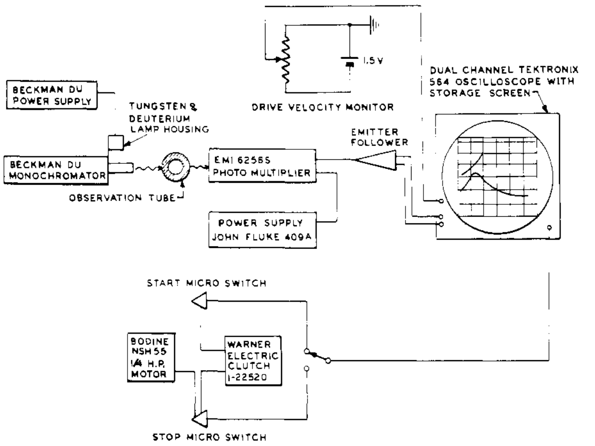

FIGURE 1: Block diagram showing connections of components of the stopped-flow spectrophotometer.

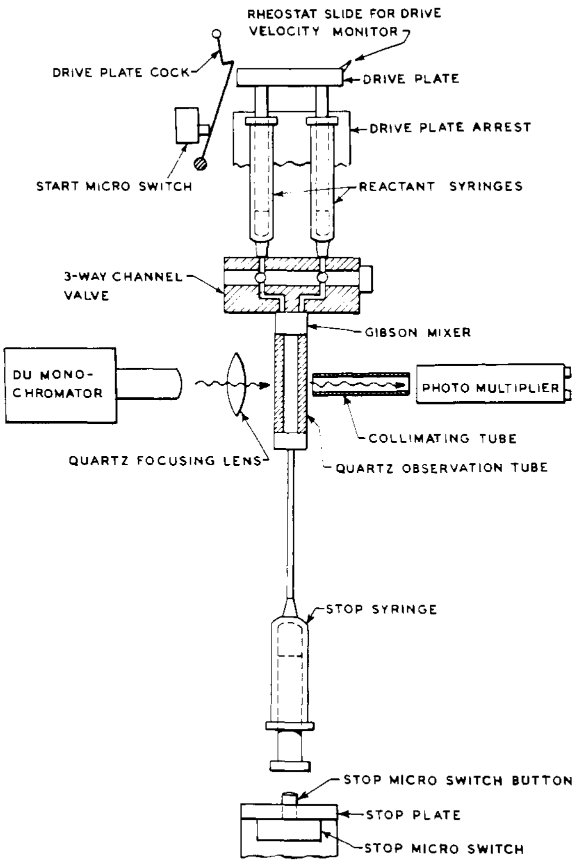

FIGURE 2: Schematic diagram showing the layout of the mechanical and optical components of the stopped-flow spectrophotometer. In the actual apparatus the needle connecting the observation tube to the stop syringe is curved through a right angle so that the stop syringe is horizontal.

As a test of the response of the apparatus the kinetics of alkaline hydrolysis of 2,4-dinitrophenyl acetate was measured in the range from 0.05 to 0.5 M in NaOH. The optical density change at 400 mμ followed first-order kinetics at each hydroxide concentration. Representative data for three concentrations are shown in Figure 4. A value for the second-order rate constant of 52 M^{-1} sec^{-1} at 23° was obtained which agrees reasonably well with the value of 49.5 M^{-1} sec^{-1} at 25° reported by Barman and Gutfreund (1963).

The effect of viscosity on mixing time was tested by variation of the viscosity by the addition of sucrose and by changing the temperature. The mixing of

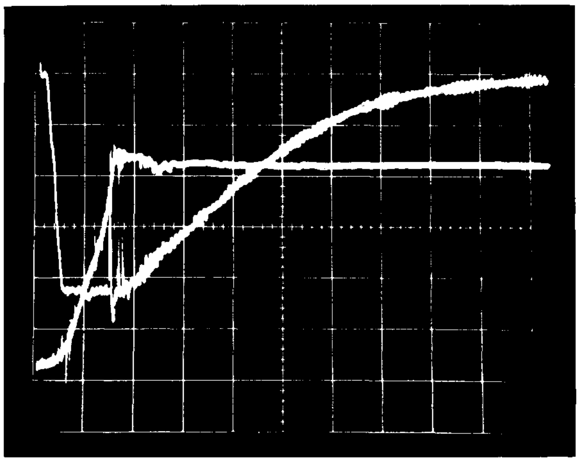

FIGURE 3: Oscilloscope pattern illustrating mixing in the stopped-flow spectrophotometer. The trace beginning from the lower left records the displacement of the drive syringe. The slope of the curve is proportional to flow velocity in the observation tube. The second trace is the photomultiplier signal obtained from the dehydration of carbonic acid with bromophenol blue as pH indicator. The initial falling phase arises from washing out of solution from the previous experiment. It should be noted that the photomultiplier signal becomes constant even before the drive stops indicating that washout and mixing is complete. Oscilloscope sweep was triggered by start microswitch.

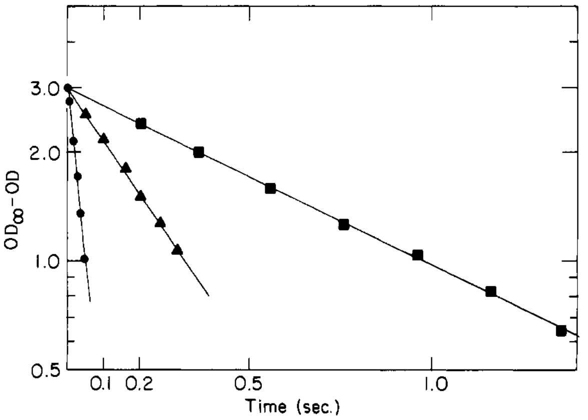

FIGURE 4: Alkaline hydrolysis of 2×10^{-5} M 2,4-dinitrophenyl acetate, 23°, wavelength 400 mμ at (—●—) 0.5 M NaOH, (—▲—) 0.1 M NaOH, and (—■—) 0.07 M NaOH. Optical density scale in arbitrary units.

bromophenol blue with 0.1 N HCl was essentially complete before solution reaches the observation tube for viscosities up to 11–12 cP. At this viscosity the delivery time was 1.3 msec. For higher viscosities mixing efficiency decreases rapidly. At 20 cP, 10 msec was required to obtain 95% mixing. Since the viscosities of myosin solutions were much less than 10 cP, the dead time of the apparatus is a few milliseconds.

Reduction of Data. The trace of the storage oscilloscope was photographed on Polaroid type 57 film by a C-12 Tektronics oscilloscope camera. Xerox reproductions of the pictures were used for measurement of displacements of the trace relative to base line. Reactions were followed over a period of at least 3 half-lives. Because changes in transmission were less than 5% of initial transmission the approximation

$$\Delta OD = \log \frac{V_i + \Delta V}{V_i} \cong 0.434 \frac{\Delta V}{V_i}$$

was used, where V_i is the initial voltage. ΔV and ΔOD are the changes in voltage and optical density at time, t, respectively. The error introduced by this approximation is less than 1%, and it greatly facilitates handling of large quantities of data.

Measurement of pH Change. The experimental results consisted in all cases of a relatively rapid liberation of protons compared with the rate in the steady state. The steady-state rate was determined at long times and a new base line was established by extrapolating this slow change back to zero time. A standard procedure was adopted, of using the time range from the 9th to 12th half-lives of the rapid reaction to establish the base line. The resulting $\Delta V/V_b$, where V_b is the corrected initial voltage, was fitted to sums of exponentials by a procedure described in the Results section. It should be emphasized that determinations of the rate constants of the exponential terms do not depend upon the calibration of voltage change in pH units as long as ΔV is linear in ΔpH, and this condition was satisfied for the pH changes associated with the presteady-state phase of the reaction.

Determination of the magnitude of the proton liberation depends upon the buffer capacities of the reagents and upon calibration of the optical path length of the apparatus.

The relation between changes in pH and optical density was determined by titration of the dye. The pK of the dye varies nearly linearly with temperature from 8.25 at 0° to 8.07 at 30°. For a range of approximately ±0.1 pH unit at pH 8 optical density varies linearly with pH. Thus the quantity $(1/OD_0)\cdot\Delta OD/\Delta\text{pH}$ is a constant over this range and its value was determined from measurements made in the Cary 14 spectrophotometer; $OD_0 = l\epsilon C_0$, where l is optical path length, C_0 is molar concentration of the dye, and ϵ is its molar extinction coefficient in the basic form. ϵ showed a small variation with temperature ($\epsilon = 7.01 \times 10^4$ M^{-1} cm^{-1} at 20° and 7.35×10^4 M^{-1} cm^{-1} at 0°). Using the equivalent path length in the stopped-flow apparatus one obtains $\Delta\text{pH} = (0.42 \times 10^{-6}/C_0)\Delta OD$ at 20°.

The buffer capacity of myosin was determined by titration in 0.5 M KCl at 0 and 23° and in the presence or absence of 0.01 M $MgCl_2$ or 0.01 M $CaCl_2$. At 23° and with no divalent ion added, the capacity expressed as moles of hydrogen ion absorbed per unit change in pH at pH 8 is 16 (myosin), where myosin concentration is expressed in moles per liter. In most experiments myosin contributed 60–80% of the buffer capacity. In the presence of Mg or Ca ion, the capacity was about 30% less at pH 8. The contribution of the nucleotide was negligible; the remaining buffer capacity was due to the dye itself, and is determined from the optical density change. Denoting the dye reaction by $H^+ + I_n = HI_n$, the absorption of protons by the dye is $\Delta[HI_n] = \Delta OD/\epsilon l$. Combining these contributions gives for the moles of protons liberated per liter, $\Delta[H^+] = 16(\text{myosin})\Delta\text{pH} + 0.77 \times 10^{-4}\,\Delta OD + \Delta[H_f{}^+]$ at 20° and pH 8, where $\Delta[H_f{}^+]$ is the increase in molar concentration of free hydrogen ion.

As an example of the values in a typical experiment the dye concentration was 5.6×10^{-6} M and myosin was present at 2 mg/ml (4×10^{-6} M). The optical density change during the transient period was 0.85×10^{-2}. Therefore $\Delta\text{pH} = 2.35\,\Delta OD = 2 \times 10^{-2}$ and $\Delta[H^+] = 1.28 \times 10^{-6} + 0.65 \times 10^{-6} + 0.0005 \times 10^{-6} = 1.93 \times 10^{-6}$ M. Proton liberation per mole of myosin was 0.48. About two-thirds of the protons liberated in the reaction are reabsorbed by the buffer capacity of the myosin and about one-third by the buffering of the dye while the change in free hydrogen ion concentration is negligible in comparison.

As the evaluation of $\Delta[H^+]$ per mole depends upon correction of experimental data for the steady-state rate, measurements of ϵ, l, and the concentrations and buffer capacities of myosin and dye, the accumulation of errors could lead to an uncertainty of 25%.

The calibration was also checked internally by comparing the steady-state rate of ATP hydrolysis in the stopped-flow apparatus with the determination of phosphate liberation from the same sample. At pH 8 one proton is produced per mole of ATP hydrolyzed. The ratio of proton liberation to phosphate liberation was 1.08 ± 0.13 indicating that the calibration was essentially correct.

Enzymatic activity of myosin appeared to survive the mixing procedure reasonably well. Rate of phosphate liberation with MgATP or CaATP as substrate was reduced by about 15% by passage of myosin through the mixer. At least part of the loss is due to cavitation bubbles formed in the stop syringe which would not contribute losses to the reaction seen in the observation tube.

No detectable optical changes occurred when myosin and *o*-cresosol sulfonephthalein or MgATP and *o*-cresosol sulfonephthalein were mixed in the apparatus. Mixing myosin–dye solution with ATP–dye solution (the normal procedure) but in the presence of 0.01 M Tris buffer to suppress any pH change also failed to produce any optical density variation. Since solutions are completely mixed before reaching the observation tube, any transients due to differences in

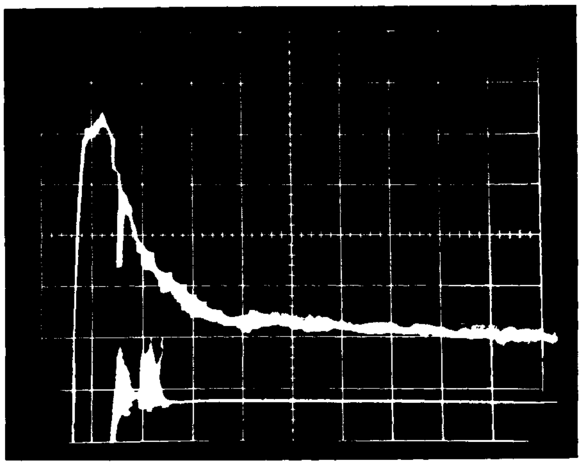

FIGURE 5: Proton liberation in the reaction of MgATP with myosin. Lower trace is piston displacement and upper one is photomultiplier signal. The rising phase of the photomultiplier signal arises from washout of solution from the previous experiment. The scale is 20 mV/major vertical division and 50 msec/major horizontal division; 4.2μ M myosin, 0.1 mM ATP, 3 mM $MgCl_2$, 0.5 M KCl, and 56 μM *o*-creosol sulfonephthalein, pH 8.0, 18.4°, λ 572 mμ.

pH of the two solutions or to protein–dye interactions are either complete or have no detectable kinetic effects.

Results

Proton Liberation with MgATP as Substrate. The change in pH from myosin–substrate reactions consisted in all cases of proton liberation. A typical oscilloscope trace obtained with MgATP as substrate is shown in Figure 5. The oscilloscope sweep was triggered at the beginning of piston displacement which is recorded on the lower trace. The rising phase of the photomultiplier signal, which occurs during piston displacement, is caused by the presence in the observation tube at zero time of solution from the previous experiment. Changes in the reaction mixture, which is 1–3-msec old, when it reaches the observation tube are observed after the piston stops and it is evident that only a proton liberation phase is detectable and that the rate is much faster than the steady-state rate. This type of behavior will be referred to as a proton early burst since the expected behavior for a simple reaction is a lag phase during which the rate increases to its steady-state value.

Since the expected analytical solution of kinetic equations, if the substrate concentration is constant, is a sum of exponentials, the data was fitted to one or more exponential terms by a graphical procedure. The quantity $V - V_b$, where V_b is base-line voltage corrected for steady-state rate, was plotted in the form $\log (V - V_b)$ *vs.* t. A single exponential decay should yield a straight line and this type of behavior was obtained in some cases. However a semilog plot of the response obtained with MgATP at 18.5° gave a curved plot (Figure 6). The slope at long times is constant and the curve can be expressed as $C_2e^{-\lambda_2 t}$. The quantity $V - V_b$ *vs.* $C_2e^{-\lambda_2 t}$ when plotted semilogarithmically yields a straight line which can be expressed as $\Phi = Ce^{-\lambda_1 t}$ (Figure 7).

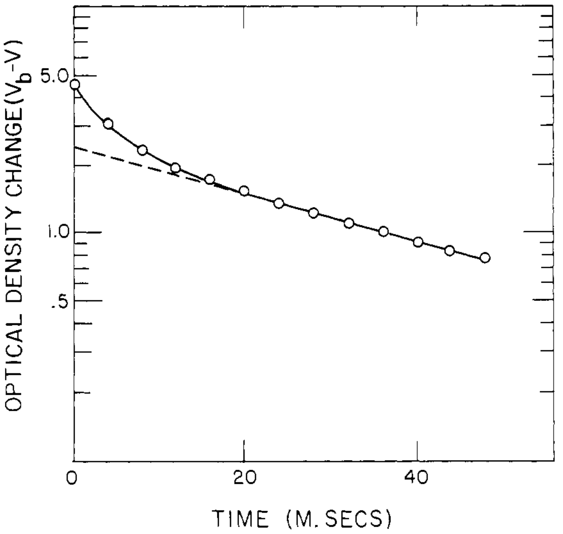

FIGURE 6: Semilog plot of voltage change in reaction of MgATP with myosin. V_b is the base-line voltage corrected for the steady-state rate; 3.7 μM myosin, 0.4 mM ATP, 19 mM $MgCl_2$, and 56 μM *o*-creosol sulfonephthalein, pH 8, 18.4°.

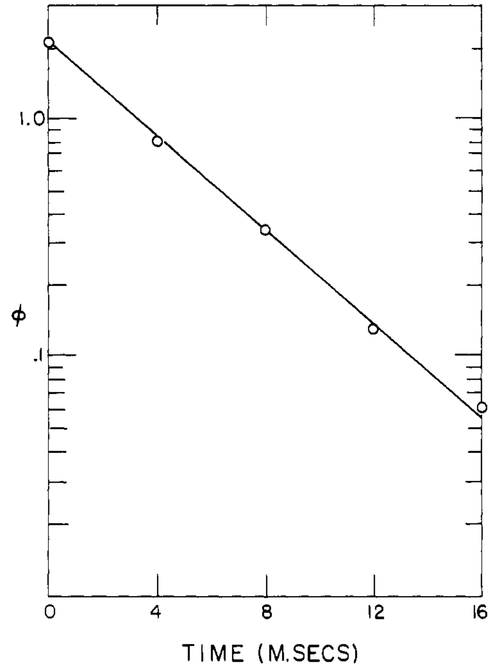

FIGURE 7: Semilog plot of Φ, the deviation from linearity shown in the curve of Figure 6. For details, see text.

In all experiments the voltage change could be represented by the decay of either one or two exponential terms. Since the parameter λ_i has dimensions of sec^{-1}, it will be referred to as a rate constant, although it can be equated to a first-order chemical rate constant only under certain conditions.

The values of λ_1 and λ_2 at 18.5° were found to vary with concentration of MgATP. The variation is shown

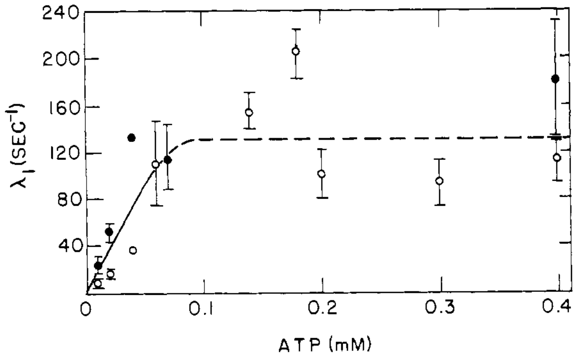

FIGURE 8: Variation of the rate constant, λ_1, with MgATP concentration. Data from two different myosin preparations are included. The error bars indicate the average deviations of duplicate or triplicate determinations. The dashed line is the least-squares fit to all data for ATP concentrations greater than 0.05 mM; 3.7 μM myosin, 0.5 M KCl, 56 μM *o*-creosol sulfonephthalein, and 3 mM $MgCl_2$, pH 8.0, 18.5°.

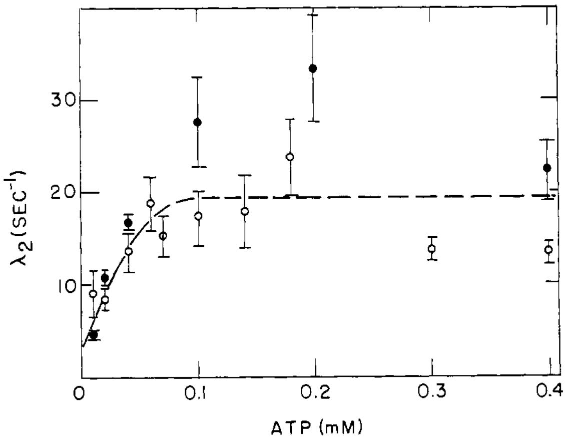

FIGURE 9: Variation of the rate constant, λ_2, with MgATP concentration, for two different myosin preparations. Conditions are the same as in Figure 8.

in Figures 8 and 9. Although the experimental errors are relatively large, the rate constants increase with concentration in the range from 10^{-5} to 10^{-4} M. At higher concentrations the λ's did not change appreciably, either reaching a plateau or decreasing at high substrate concentrations. The horizontal dashed lines in Figures 8 and 9 are the least-squares values of all determinations at concentrations greater than 5×10^{-5} M MgATP, and gave values of 130 and 20 sec^{-1}. In the concentration-dependent region the slopes of the plots, which have the dimensions of second-order rate constants, are 2×10^6 and 2.5×10^5 M^{-1} sec^{-1}.

The ratio C_2/C_1 which is the relative magnitude of the two proton steps had an average value of 2.8 ± 1.5 but because of the large scatter no consistent variation with concentration was detectable. The magnitude of the fast proton will also be underestimated by 10–30% at high concentrations because of the extent of reaction when solution reaches the observation tube.

The variation of λ_i with magnesium concentration

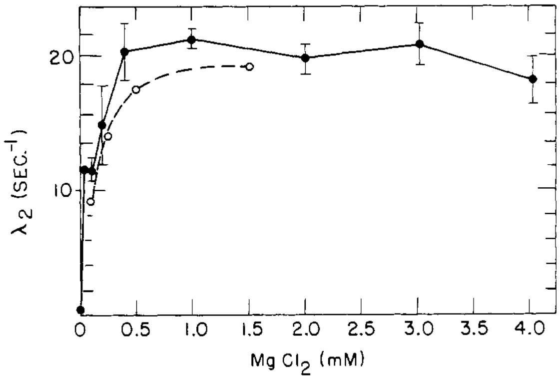

FIGURE 10: Variation of rate constant, λ_2, with magnesium concentration for a constant ATP concentration of 0.1 mM. The dashed curve was computed from the assumption that λ_2 is proportional to MgATP concentration using stability constant given by Khan and Martell (1966); 4.2 μM myosin, 0.5 M KCl, and 56 μM *o*-creosol sulfonephthalein, pH 8.0, 18.4°.

was investigated for a constant ATP concentration of 10^{-4} M. This value was chosen since the rate constants began to decrease as substrate concentration was reduced below this level. In the range from 4×10^{-3} to 10^{-5} M $MgCl_2$ there was no consistent variation in λ_1; the average value was 107 ± 54 sec^{-1}. λ_2 was constant for $MgCl_2$ concentrations greater than 5×10^{-4} M but decreased sharply at lower concentrations (Figure 10). The dashed curve in the figure was calculated on the assumptions that the true substrate is MgATP using the stability constant ($\log K = 4.16$) given by Khan and Martell (1966) and a linear concentration dependence of λ_2 computed from the data shown in Figure 9, *i.e.*, $\lambda_2 = 2.5 \times 10^5$ (MgATP). The curve for λ_2 lies to the left of the calculated curve, *i.e.*, it corresponds to a slightly larger stability constant. The Khan and Martell data was obtained in 0.1 M KNO_3 and if an approximate correction is made for potassium binding using a value of 9 for the KATP stability constant (Botts *et al.*, 1965), the apparent MgATP constant is reduced to 3.6–3.7 and the discrepancy is larger. Therefore although Mg is required for the slower proton step the apparent binding constant is somewhat larger than expected for a complex with free nucleotide.

At 0°, MgATP yielded a proton early burst represented by a single rate constant which increased linearly with concentration in the range from 10^{-5} to 2×10^{-3} M with no indication of a plateau (Figure 11).

The magnitude of the proton early burst for MgATP at 18° increased with concentration up to about 2×10^{-4} M (Figure 12). The maximum value attained was about 0.6 mole/mole. This estimate may be about 10% too low due to partial reaction before the sample reaches the observation tube. In view of the errors inherent in the calibration procedure the total proton release could be as large as 1 mole/mole. The actual pH change in all experiments was quite small and did not exceed 0.02 pH unit.

Proton Liberation with CaATP and MgITP as Substrate. The much larger steady-state rate of hydrolysis

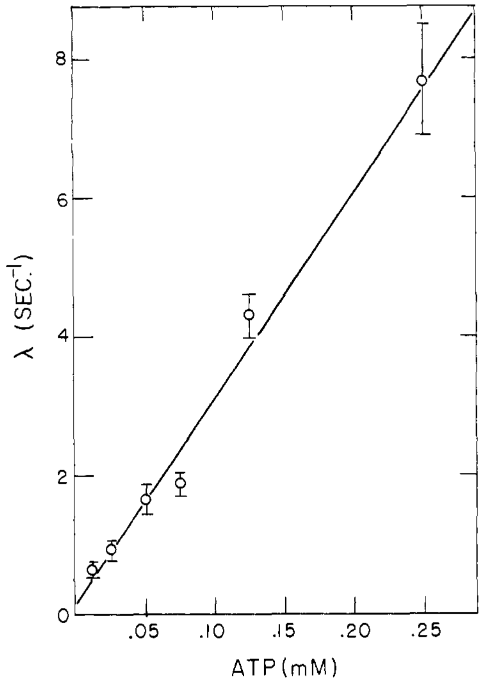

FIGURE 11: Variation of rate constant for proton liberation with the concentration of MgATP at 0°; 1.8 μM myosin, 10 mM $MgCl_2$, 0.5 M KCl, and 56 μM *o*-creosol sulfonephthalein, pH 8.0.

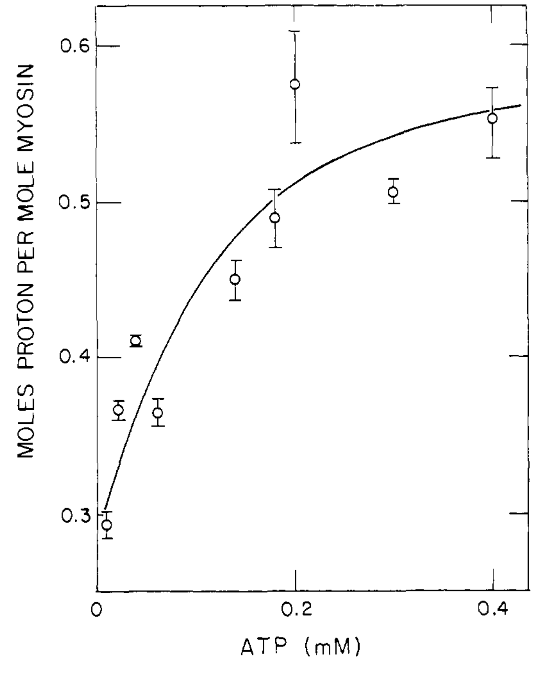

FIGURE 12: Magnitude of the early proton liberation as a function of the concentration of ATP; 3.7 μM myosin, 0.5 M KCl, 5 mM $MgCl_2$, and 56 μM *o*-creosol sulfonephthalein, pH 8.0, 18.5°.

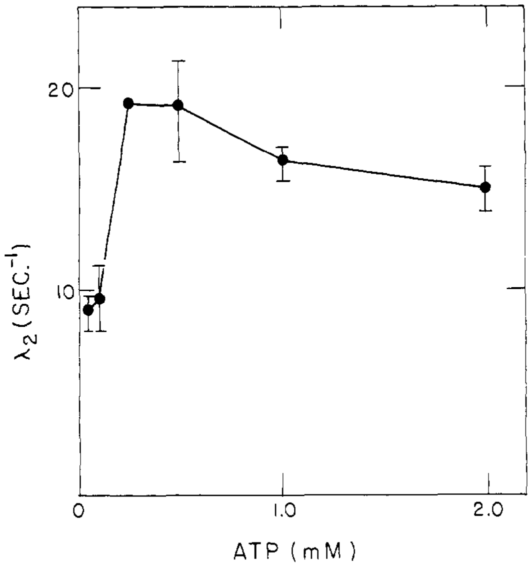

FIGURE 13: Variation of the rate constant, λ_2, with CaATP concentration, 2.6 μM myosin, 15 mM $CaCl_2$, 0.5 M KCl, and 56 μM *o*-creosol sulfonephthalein, pH 8.0, 0°.

of CaATP necessitated working at 0° to avoid substrate depletion. The reaction was similar to that of MgATP at 18° in that two exponential terms were required to fit the data. At high concentrations of CaATP (2×10^{-3} M) the rate constants are $\lambda_1 = 60 \pm 10$ sec^{-1} and $\lambda_2 = 19$ sec^{-1}. In the concentration range from 5×10^{-5} to 2×10^{-3} M, λ_1 did not vary with concentration, while λ_2 increased to a maximum at 2×10^{-3} M and decreased slowly at higher concentrations (Figure 13). The data are less extensive than with MgATP and the values of the constants are subject to rather large errors. The size of the early burst was about 0.34 mole/mole.

MgITP at 20° also gave a proton early burst but the data was represented by a single rate constant, $\lambda = 8$ sec^{-1}, which was independent of substrate concentration from 2×10^{-5} to 1.4×10^{-4} M. The size of the early burst was 0.29 ± 0.03 mole per mole.

The kinetic data are summarized in Table I.

Discussion and Conclusions

The main result of this study is the measurement of a fast proton-liberating step or steps in the hydrolysis of nucleotide triphosphates by myosin. Since the early proton was found for both Mg and Ca activation, for ATP and ITP and for 0 and 20°, it appears to be a general property of the hydrolysis mechanism which is not directly correlated with the presence of a phosphate early burst. For MgATP at 20° or CaATP at 0°, two proton steps were found, while a single process was detected for MgITP at 20° and MgATP at 0°. For the different substrates the rate constants for the proton steps are 20 to 1000 times larger than the steady-state rate constants for proton liberation at pH 8.

The data given in Table I have been expressed as first- or second-order rate constants. For those cases in which a plateau was obtained at high substrate concentration it is reasonable to identify the rate constant with a first-order step in the mechanism. The second-order rate constant obtained from the slope of the rate *vs.* concentration curves at low concentrations will not,

TABLE I: Proton Liberation.[a]

Substrate	Temp (°C)	$\frac{\Delta\lambda_1}{\Delta S}$ (M^{-1} sec^{-1})	$\lambda_{1\,max}$ (sec^{-1})	$\frac{\Delta\lambda_2}{\Delta S}$ (M^{-1} sec^{-1})	$\lambda_{2\,max}$ (sec^{-1})
MgATP	18.5	2×10^6	130	2.5×10^5	20
MgATP	0	—	—	3.8×10^4	None
CaATP	0	None	60	5×10^4	20
MgITP	20	—	—	None	8

[a] All experiments were performed at pH 8 in 0.5 M KCl, MgCl 1–2 $\times 10^{-2}$ M, or 1.5 $\times 10^{-2}$ M CaCl. Subscript one is applied to the faster process when two rate constants are required to represent the data. Dashes indicate that a single rate constant was sufficient to describe the results. "None" indicates that no concentration dependence was detected, or that a maximum value was not attained in the concentration range investigated. $\Delta\lambda_i/\Delta S$ is the slope of λ_i *vs.* substrate curve at low substrate concentrations.

in general, be equal to the rate constant for substrate binding, and its significance must be determined with reference to a particular kinetic scheme.

With MgATP as substrate the extent of the early proton liberation at 18° was 0.6–0.7 mole per 5×10^5 g, which we assume to be the molecular weight of myosin. With MgITP and CaATP the figure was about 0.3 mole/mole. Since the figure depends upon calibration of the pH change, the possible error is relatively large. The value could range from 0.5 to nearly 1 for MgATP at 18°, but for MgATP at 0°, MgITP and CaATP the figure is definitely less than 1 mole.

Tonomura *et al.* (1962) found by measurements in a Titrigraph or a rapidly responding pH meter that proton liberation was linear with time and passed through the origin. However, it is doubtful whether the fast proton liberation described here could be observed by direct pH determinations. The total change which was generally less than 0.02 pH unit was completed in a few tenths of a second in the stopped-flow apparatus. To measure this change with a pH meter, since it occurs as fast as reagents are mixed, would require adjustment of the pH of the ATP and myosin solutions to the same value with an accuracy much better than 0.02 pH unit.

A detailed kinetic scheme for the hydrolysis of MgATP has been proposed by Tonomura and collaborators (Kanazawa and Tonomura, 1965; Tokiwa and Tonomura, 1965; Imamura *et al.*, 1965, 1966; Nakamura and Tonomura, 1968) and since the present results are not in agreement with their findings it is necessary to briefly discuss their model (eq 1).

We are concerned primarily with the proton steps although it should be noted that their scheme is also designed to explain the phosphate early burst by formation of the complex $E_1 \cdot P$. The model is based on the finding of the absorption of one proton (step k_3) followed by the liberation of one proton (step k_4) with rate constants of 18 and 4.5 sec^{-1}, respectively. The values of k_3 and k_4 were reported for only a single concentration of MgATP.

In the experiments described here no proton absorption step was found for any conditions of temperature, ion activation, or substrate. For 10^{-4} M ATP, 10^{-3} $MgCl_2$, which corresponds to the values used by Tonomura, we find proton liberation with rate constants of 130 and 20 sec^{-1} in a total amount which was less than 1 mole/mole. The reason for this discrepancy is not known although it should be noted that an apparent proton absorption would be seen if at $t = 0$ mixing is incomplete or solution from the previous experiment has not been washed out of the observation tube (the effect could be simulated by displacing $t = 0$ to the left in Figure 5).

The results reported here cannot be fitted into the scheme proposed by Tonomura, yet it must be admitted that we cannot account for two proton steps as well as the phosphate early burst and ^{18}O exchange (Levy and Koshland, 1959; Levy *et al.*, 1962; Sartorelli *et al.*, 1966) by a model with fewer intermediates than are present in Tonomura's scheme. Once two enzyme–substrate complexes are introduced, as in the Tonomura mechanism, it is necessary to include the steps $E_1 \xrightarrow{\pm H^+} E_2$ and $E_2 + S \rightleftarrows E_2S$. The proton steps could therefore be associated with a change in configuration of free enzyme or enzyme–substrate complex and with the hydrolysis step itself. Solutions of the appropriate kinetic equations indicate that all of these possibilities could lead to the behavior found experimentally of a concentration-dependent range and a plateau. The second-order rate constants given in Table I would then be the rate constants for substrate binding or ratios of rate constants depending upon the mechanism assumed.

In summary, the myosin enzyme mechanism appears to involve one or two proton-liberating steps depend-

$$\begin{tikzcd}
E_1 + S \arrow[r, shift left, "k_1"] & E_1S \arrow[l, shift left, "k_{-1}"] \arrow[r, "k_2"] \arrow[d, shift left, "k_3(H^+)"] & E_1 + ADP + P_i + H^+ & & \\
& E_2S \arrow[u, shift left] \arrow[r, shift left, "k_4(-H^+)"] & E_1 \cdot P \cdot ADP \arrow[l, shift left] \arrow[r, "(-ADP)"] & E_1 \cdot P \arrow[r, "k_5"] & E_1 + P_i + H^+
\end{tikzcd} \tag{1}$$

ing upon the substrate and temperature. Although the results could be explained by introducing two enzyme–substrate complexes as postulated by Tonomura, the available evidence does not appear to justify the selection of this model in preference to other possible assignments of the proton steps. Direct measurements of the rate of substrate binding and measurements currently being made on the rate of formation of the enzyme–phosphate complex should help to resolve the uncertainty, as to the nature of the proton-liberating steps.

References

Barman, T. E., and Gutfreund, H. (1963), *in* Rapid Mixing and Sampling Techniques, Chance, B., Eisenhardt, R. H., Gibson, Q. H., and Lonberg-Holm, K. E., Ed., New York, N. Y., Academic.

Botts, J., Chashia, A., and Young, H. L. (1965), *Biochemistry 4*, 1788.

Gibson, Q. H., and Milnes, L. (1964), *Biochem. J. 91*, 161.

Holtzer, A., and Lowey, S. (1959), *J. Am. Chem. Soc. 81*, 1370.

Imamura, K., Kanazawa, T., Toda, M., and Tonomura, Y. (1965), *J. Biochem.* (*Tokyo*) *57*, 627.

Imamura, K., Toda, M., and Tonomura, Y. (1966), *J. Biochem.* (*Tokyo*) *59*, 280.

Kanazawa, T., and Tonomura, Y. (1965), *J. Biochem.* (*Tokyo*) *57*, 604.

Khan, M. M. T., and Martell, A. E. (1966), *J. Am. Chem. Soc. 88*, 668.

Levy, H. M., and Koshland, D. E., Jr. (1959), *J. Biol. Chem. 234*, 1102.

Levy, H. M., Ryan, E. M., Spinghorn, S. S., and Koshland, D. E., Jr. (1962), *J. Biol. Chem. 237*, 1730.

Nakamura, H., and Tonomura, Y. (1968), *J. Biochem.* (*Tokyo*) *63*, 279.

Nanninga, L. B., and Mommaerts, W. F. H. M. (1960), *Proc. Natl. Acad. Sci. U. S. 46*, 1166.

Sartorelli, L., Fromm, H. J., Benson, R. W., and Boyer, P. D. (1966), *Biochemistry 5*, 2877.

Sturtevant, J. M. (1963), *in* Rapid Mixing and Sampling Techniques, Chance, B., Eisenhardt, R. H., Gibson, Q. H., and Lonberg-Holm, K. E., Ed., New York, N. Y., Academic.

Tausky, H. H., and Shorr, E. (1953), *J. Biol. Chem. 202*, 675.

Tokiwa, T., and Tonomura, Y. (1965), *J. Biochem.* (*Tokyo*) *57*, 616.

Tonomura, Y., Kitagawa, S., and Toshimura, J. (1962), *J. Biol. Chem. 237*, 3660.